Title

NEW BETA-DELAYED PROTON EMITTERS IN THE LANTHANIDE REGION

Authors

Nitschke, J.M.
Cable, M.D.
Zeitz, W.-D.

Publication Date

1983-05-01

LBL-15895
Preprint

Lawrence Berkeley Laboratory
UNIVERSITY OF CALIFORNIA

Submitted to Zeitschrift für Physik

NEW BETA-DELAYED PROTON EMITTERS IN THE LANTHANIDE REGION

J.M. Nitschke, M.D. Cable, and W.-D. Zeitz

May 1983

NUCLEAR SCIENCE DIVISION

Prepared for the U.S. Department of Energy under Contract DE-AC03-76SF00098

LBL-15895

New Beta-Delayed Proton Emitters in the Lanthanide Region

J.M. Nitschke, M.D. Cable

Nuclear Science Division
Lawrence Berkeley Laboratory
University of California
Berkeley, CA 94720

W.-D. Zeitz

Hahn-Meitner-Institut für Kernforschung
Berlin GmbH
Bereich Kern- und Strahlenphysik
Berlin, West Germany

This work was supported by the Director, Office of Energy Research, Division of Nuclear Physics of the Office of High Energy and Nuclear Physics of the U.S. Department of Energy under Contract DE-AC03-76SF00098.

Abstract:

Several new beta-delayed proton emitters have been observed at the on-line mass separator OASIS. They were provisionally identified as: ^{125}Ce (8.9 + 0.7 s), ^{126}Pr (3.2 ± 0.6 s), ^{127}Nd (1.9 ± 0.4 s), ^{128}Nd (4 ± 2 s), ^{137}Gd (7 ± 3 s), ^{139}Gd (4.9 ± 1 s), and ^{143}Dy (4.1 ± 0.3 s).

Following the discovery of proton radioactivity from the ground state, a search for other proton emitters was undertaken using the on-line isotope separator OASIS [1]. Gas-cooled targets (1-2 mg/cm^2) of ^{92}Mo, ^{90}Zr, ^{54}Fe, and ^{50}Cr were bombarded with beams of ^{92}Mo, ^{58}Ni, ^{56}Fe, and ^{40}Ca ($5 \cdot 10^{10}$–$2 \cdot 10^{12}$ s^{-1}) from the SuperHILAC. The target recoils were stopped in the tantalum catcher of a high-temperature surface ionization source operated at about 2700 C. After mass separation the ion beam of the selected mass was deflected electrostatically toward one of two proton telescopes, with the deflection period matched to the expected half-life. Half-lives were calculated from growth and decay data using the maximum likelihood method. The proton telescopes consisted of thin ΔE detectors (10 and 28 μm) and "thick" E detectors (430 and 1040 μm).

Predictions in [2] indicate that several isotopes in the lanthanide region should have proton branches and half-lives so as to be observable. Three isotopes, in addition, can be produced with cross sections in the 10^{-29}cm^2 range: ^{143}Ho, ^{137}Tb, and ^{127}Pm. No ground state proton emission, characterized by sharp proton lines, was found, but broad proton energy spectra characteristic of delayed proton emission were observed. The insert of fig. 1 shows a typical example. In all experiments the mass of the selected isotope was unequivocally established by extrapolation from known, stable masses with an NMR mass meter. The Z identificaton in several cases is less certain and was based on a comparison between the observed and predicted values of three parameters: (a) the half-life calculated from the gross theory of β-decay [3], (b) the production cross section calculated with the code ALICE [4], and (c) the predicted difference between electron-capture Q-value and proton separation energy ($Q_{EC}-S_p$) as a function of

Z, using the Liran-Zeldes mass predictions [5] (fig. 2). The usefulness of cross-section predictions is, however, compromised by the inherent uncertainty in their calculation and the unknown proton branching ratios. In some cases, cross bombardments have helped to narrow down the Z-assignment. This procedure can best be explained with an example: In the bombardment of ^{90}Zr with 182 MeV ^{40}Ca ions, protons of 2.1 to 5.0 MeV energy, decaying with a half-life of 3.2 ± 0.6 s, were observed at mass 126. For A = 126, fig. 2 shows that the condition $(Q_{EC} - S_p) - \Theta_p >> 0$ (where Θ_p is the effective proton emission threshold) is fulfilled for Z = 59 (Pr) and Z = 60 (Nd). The calculated cross sections for $^{90}Zr(^{40}Ca,4n)^{126}Nd$ and $^{90}Zr(^{40}Ca,p3n)^{126}Pr$ are 20 μb and 4 mb respectively. The predicted half-lives are 2 s for ^{126}Nd and 3 s for ^{126}Pr. From the longer half-life and the much larger cross section, it can be concluded that the observed activity is most likely ^{126}Pr.

The following comments pertain to the assignments in Table 1.

A = 124: This experiment was undertaken to search for delayed proton emission from ^{124}La. In two separate bombardments with 182 and 196 MeV ^{40}Ca ions on ^{90}Zr no protons were observed. From fig. 2 it can be deduced that the next possible A = 124 proton emitter is ^{124}Pr, for which the optimum bombarding energy is, however, 230 MeV. In the present experiment ^{124}Pr would have been produced with a cross section of only 1 μb and would therefore have been unobservable.

A = 125: The preliminary assignment for the delayed proton precursor at this mass is ^{125}Ce, which was first identified via x-ray analysis and has a half-life of 11 ± 4 s [6]. This agrees well with the proton half-life of 8.9 ± 0.7 s observed in the present experiments and the calculated half-life for ^{125}Ce of 10 s [3].

A = 127: The observed proton spectrum shown in fig. 1 (insert) is typical for delayed proton emission. From the growth and decay data, a half-life of 1.9 ± 0.4 s was deduced, which is in good agreement with the calculated value of 1.8 s for ^{127}Nd [3]. The proton energy distribution from 2.0 to 6.4 MeV was also observed in a "cross bombardment" with ^{40}Ca on ^{90}Zr albeit with much lower yield.

A = 128: In this case poor statistics resulted in a large error for the half-life (4 ± 2 s). The low maximum proton energy of 4.5 MeV indicates that either ^{128}Nd or ^{128}Pr is being observed. The predicted half-lives for these two isotopes are 6.4 and 8.3 s, respectively, which favors the ^{128}Nd interpretation; some contribution from ^{128}Pr can, however, not be excluded.
A = 137: A wide distribution of proton energies that decayed with a half-life of 7 ± 3 s was found. As in the case of A = 128 a more precise value for the half-life will have to be determined in a later experiment. Figure 2 gives two possible candidates for this activity, Tb and Gd; however, the 100 times larger cross section and the longer, calculated half-life of 2 s (vs. 0.64 s for ^{137}Tb) point to ^{137}Gd as the correct assignment.
A = 139: The identification of this isotope as ^{139}Gd is well supported by the ($Q_{EC} - S_p$) value of 6.50 MeV, a large cross section of 70 mb, and the good agreement between the experimental half-life of 4.9 ± 1.0 s and the calculated value of 6.4 s [3]. In a cross bombardment with ^{92}Mo on ^{54}Fe, protons in the same energy range as in the ^{50}Cr + ^{92}Mo case were observed although with much lower yield due to a fivefold reduction in cross section.
A = 143: In two experiments with ^{58}Ni and ^{56}Fe beams on ^{92}Mo targets, beta-delayed protons with similar half-lives and similar energy distributions were observed. The weighted average half-life of 4.1 ± 0.3 s is in agreement with the calculated value of 3.2 s for ^{143}Dy. ^{143}Ho as precursor can be excluded because of the 100 times lower production cross section and the shorter theoretical half-life of 1.0 s.

This work was supported by the Director, Office of Energy Research, Division of Nuclear Physics of the Office of High Energy and Nuclear Physics of the U.S. Department of Energy under Contract DE-AC03-76SF00098.

Table 1: Target-projectile combinations and provisional reaction channels for the production of beta-delayed proton precursors. E_{Lab} = bombarding energy, E_p = observed proton energy range, $\bar{E}_p$ = centroid of the proton spectrum, and $T_{1/2}$ = half-life of the precursor.

Reaction	E_{Lab} (Mev)	E_p (MeV)	$\bar{E}_p$ (Mev)	Precursor	$T_{1/2}$ (s)
^{90}Zr(^{40}Ca,αpn)	196	no protons		(^{124}La)	-
^{90}Zr(^{40}Ca,αn)	196	2.0-4.7	(3.4)	^{125}Ce	8.9±0.7
^{90}Zr(^{40}Ca,p3n)	182	2.1-5.0	(3.8)	^{126}Pr	3.2±0.6
^{92}Mo(^{40}Ca,αn)	213	2.0-6.4	(3.7)	^{127}Nd	1.9±0.4
^{92}Mo(^{40}Ca,α)	188	2.1-4.5	(3.3)	^{128}Nd	4 ±2
^{50}Cr(^{92}Mo,αn)	480	2.2-6.6	(3.8)	^{137}Gd	7 ±3
^{50}Cr(^{92}Mo,2pn)	385	2.1-5.5	(3.8)	^{139}Gd	4.9±1.0
^{92}Mo(^{58}Ni,α2pn)	292	2.1-6.4	(4.2)	^{143}Dy	4.3±0.3
^{92}Mo(^{56}Fe,αn)	275	2.0-5.6	(4.1)	^{143}Dy	3.7±0.7

References

1. J.M. Nitschke, Nucl. Inst. and Meth. 206, 341 (1983)
2. W.F. Feix and E.R. Hilf, Darmstadt, IKDA 82/12
3. K. Takahashi, M. Yamada, T. Kondoh, Atomic and Nucl. Data Tables 12, 101 (1973)
4. M. Blann and J. Bisplinghoff, UCID-19614
5. S. Liran and N. Zeldes, Atomic and Nucl. Data Tables 17, 431 (1976)
6. D.D. Bogdanov, A.V. Demyanov, V.A. Karnaukhov, M. Nowicki, L.A. Petrov, J. Voboril, and A. Plochocki, Nucl. Phys. A305, 421 (1978)

Figure Captions

Fig. 1: Growth and decay curve of the delayed proton activity at mass 127. The activity was accumulated on each telescope for 20 s and its decay observed for another 20 s. The data from both telescopes were combined. The insert shows the proton energy spectrum.

Fig. 2: (Q_{EC} - S_p) and Θ_p as functions of Z for constant A. Q_{EC} = Q-value for electron capture of the delayed proton precursor (Z,A), S_p = proton separation energy of the delayed proton emitter (Z-1,A), and Θ_p = threshold for proton emission. The shaded areas indicate schematically the energy range of the observed protons. The underlined Z-values denote the preliminary assignment of the precursor.

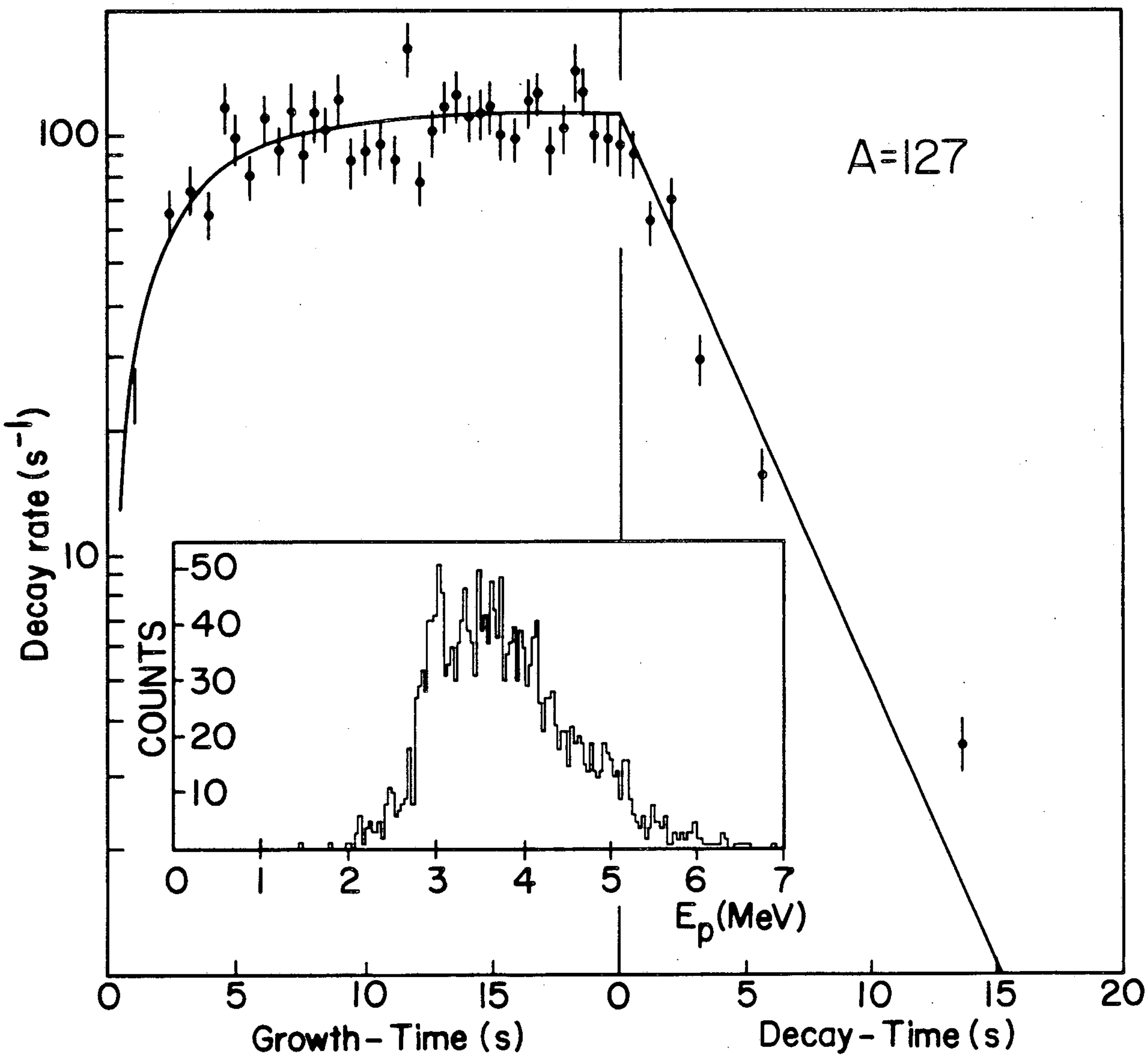

XBL 835-9514

Fig. 1

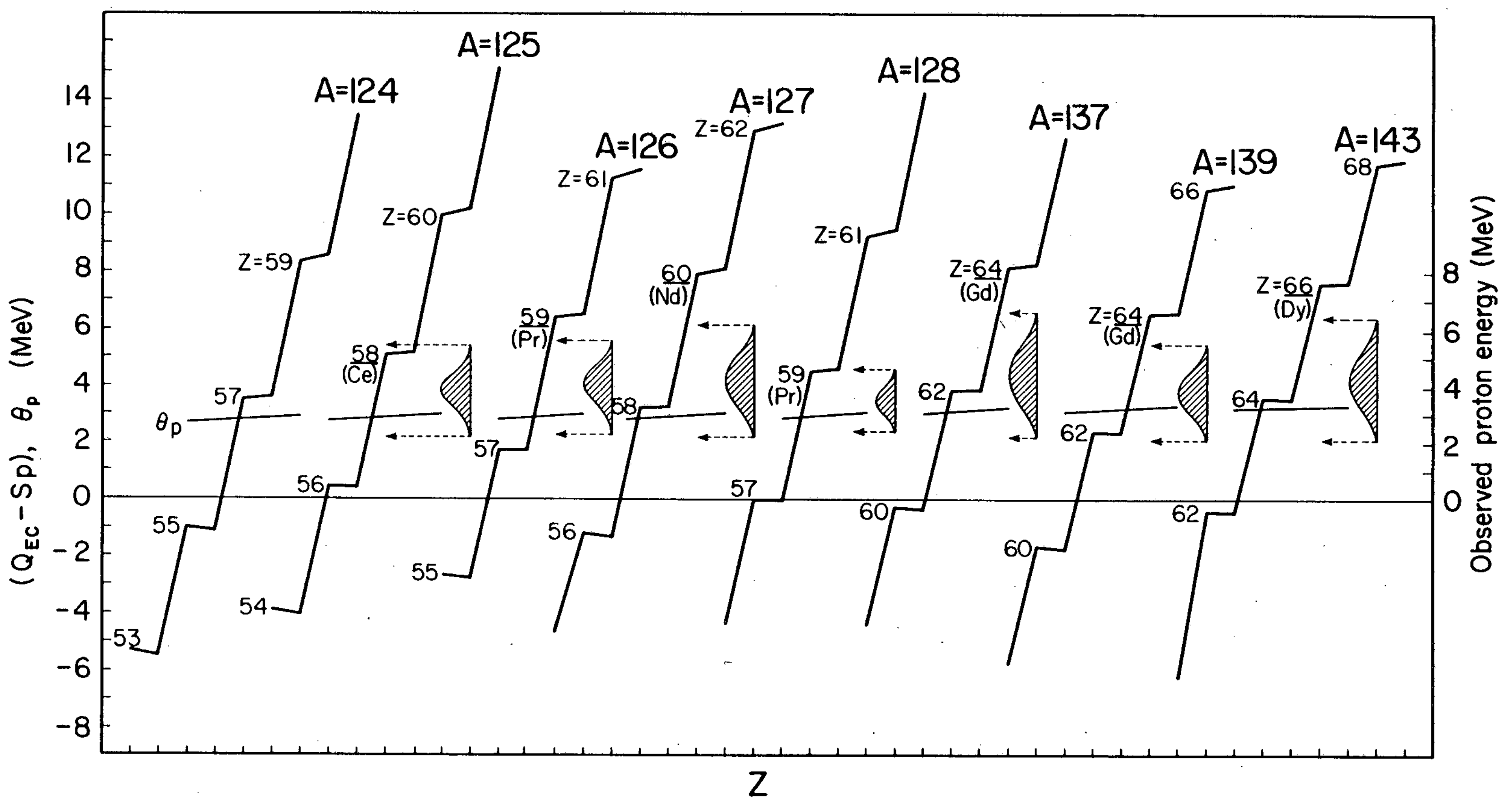

XBL 835-9512

Fig. 2

TECHNICAL INFORMATION DEPARTMENT
LAWRENCE BERKELEY LABORATORY
UNIVERSITY OF CALIFORNIA
BERKELEY, CALIFORNIA 94720